

## Unusual structure and magnetism in manganese oxide nanoclusters

Shreemoyee Ganguly,<sup>1</sup> Mukul Kabir,<sup>2,\*</sup> Biplab Sanyal,<sup>3</sup> and Abhijit Mookerjee<sup>1</sup>

<sup>1</sup>*Advanced Materials Research Unit and Department of Materials Science, S.N. Bose National Center for Basic Sciences, JD Block, Sector III, Salt Lake City, Kolkata 700 098, India*

<sup>2</sup>*Department of Materials Science and Engineering, Massachusetts Institute of Technology, Cambridge, Massachusetts 02139, USA*

<sup>3</sup>*Department of Physics and Astronomy, Uppsala University, Box 516, SE-751 20 Uppsala, Sweden*  
(Received 15 December 2010; published 31 January 2011)

We report an unusual evolution of structure and magnetism in stoichiometric MnO clusters based on an extensive and unbiased search through the potential-energy surface within density functional theory. The smaller clusters, containing up to five MnO units, adopt two-dimensional structures; and regardless of the size of the cluster, magnetic coupling is found to be antiferromagnetic in contrast to previous theoretical findings. Predicted structure and magnetism are strikingly different from the magnetic core of Mn-based molecular magnets, whereas, they were previously argued to be similar. Both of these features are explained through the inherent electronic structures of the clusters.

DOI: [10.1103/PhysRevB.83.020411](https://doi.org/10.1103/PhysRevB.83.020411)

PACS number(s): 36.40.Cg, 71.15.Mb, 75.75.-c

Transition metal-oxide, especially MnO,<sup>1–5</sup> clusters have recently attracted extensive multidisciplinary research activity because of their diverse and tunable magnetic and catalytic properties. Generally, as compared to the bulk, the local magnetic moment is enhanced in smaller dimensions due to reduction in the number of neighboring atoms. This results in either an overall enhancement of the total moment for the ferromagnetic (FM) case or leads to a finite moment even for the antiferromagnetic (AFM) case due to unequal compensation of spin-up and spin-down electrons. Magnetic coupling also evolves with particle size, and such size evolution for MnO clusters is nonmonotonic. MnO clusters with a diameter of 5–10 nm show FM behavior,<sup>6</sup> although the bulk phase is AFM.<sup>7</sup> In contrast, Mn-based single molecular magnets (with magnetic cores < 1.5 nm) show a layered ferrimagnetic structure within the mixed-valent Mn centers, resulting in a large magnetic moment and spin anisotropy.<sup>1,2</sup> Moreover, the MnO clusters take essential part in a variety of biological (catalytic) processes from photosynthesis to bacterially mediated organic matter decomposition. The active inorganic center of the oxygen evolving photosystem II contains a manganese-oxide cluster (Mn<sub>4</sub>O<sub>4</sub>Ca), which catalyzes the light-driven oxidation of water.<sup>3</sup> Indeed, synthetic complexes containing cuboidal Mn<sub>4</sub>O<sub>4</sub> cores have been found to exhibit unique reactivity in water-oxidation/O<sub>2</sub> evolution.<sup>4</sup>

The prediction of geometry at the atomic level is one of the most fundamental challenges in condensed-matter science. The magnetic and catalytic properties (i.e., broadly speaking: the electronic structure) are strongly coupled to the inherent structure [corresponding to minima of the potential-energy surface (PES)] of the cluster. Experimental evidence of structure and magnetic coupling and their size evolution for the transition metal-oxide clusters in the gas phase are scarce. However, the structure and (FM) magnetism of (MnO)<sub>x</sub> clusters have been predicted theoretically.<sup>8–10</sup> Such a theoretical prediction is complex and requires a systematic and rigorous search through the PES. This is essential to predict the deepest minima. The complexity of the PES search increases with increasing cluster size. Possible geometrical

structures increase exponentially with cluster size, and for a given geometrical structure containing  $N$  magnetic ions, there are  $2^N$  spin configurations (which may or may not be reduced depending on the symmetry). In contrast, all the previous theoretical attempts have been largely biased<sup>8–10</sup> because: (i) Geometrical structures were restricted by a particular symmetry, and (ii) magnetic structures were restricted to the FM regime. Such limited considerations only search a small subspace of the entire PES and, thus, previously reported geometric/magnetic structures may not represent the true ground states. Indeed, in contrast to the previous theoretical reports, in this Rapid Communication we will report, based on a rigorous PES search, that the (MnO)<sub>x</sub> clusters show AFM coupling and also show unusual two-dimensional (2D) structures up to a certain size.

The spin-polarized density functional theory calculations were conducted using the VASP code<sup>11</sup> with the Perdew-Burke-Ernzerhof exchange-correlation functional<sup>12</sup> and the projector augmented wave pseudopotential<sup>13</sup> at an energy cutoff of 270 eV. Simple cubic supercells were used with periodic boundary conditions, and it was made sure that that two neighboring image clusters were separated by at least 10 Å of vacuum space. This ensured that the interaction of the cluster with its periodic image was negligible, and reciprocal space integrations were carried out at the  $\Gamma$  point. We started with high-symmetry structures, for example, a cubic structure (core of the Mn<sub>12</sub>-molecular magnet<sup>1</sup>) for the (MnO)<sub>4</sub> cluster. Spin-polarized Born-Oppenheimer molecular dynamics (BOMD) simulations at 1200 K were performed for 20–30 ps to search for the lowest energy isomers. This approach could efficiently explore the PES. Several minimum-energy structures were then picked from these BOMD simulations and were carefully restudied. All of these minimum-energy structures were further optimized (*local* ionic relaxation) with all possible spin multiplicities. Moreover, we have also considered different spin arrangements for different atoms in the cluster for a particular spin multiplicity.

Although the magnetic structure is strongly coupled with cluster geometry, we first discuss the geometric evolution

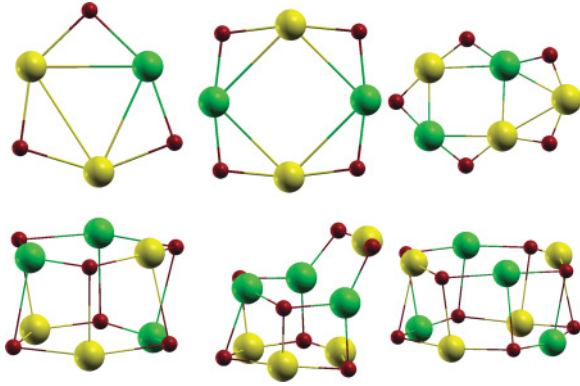


FIG. 1. (Color online) Geometrical evolution shows a 2D to three-dimensional (3D) transition at  $(\text{MnO})_6$ . Minimum-energy structures are always found to be AFM. The up (down) Mn atoms are shown with yellow/light gray (green/gray) color. Oxygen atoms are shown in red/dark gray. The Mn-O (1.80–2.18 Å) and Mn-Mn (2.55–3.10 Å) distances and the Mn-O-Mn angles ( $78^\circ$ – $108^\circ$ ) in these clusters are comparable to the Mn-based molecular magnets.<sup>1,2</sup>

alone. For the MnO dimer, as expected, the Mn-O distance is much smaller (1.65 Å) than bulk, in agreement with experimental<sup>14</sup> and diffusion quantum Monte Carlo (DMC) results.<sup>15</sup> Calculated Mn-O stretching frequency ( $920\text{ cm}^{-1}$ ) is slightly higher than the experimentally obtained values [ $832\text{ cm}^{-1}$  (Ref. 14) and  $899\text{ cm}^{-1}$  (Ref. 16)] in the gas phase. The average Mn-O distances increase with cluster size, and the lowest energy structures are shown in Fig. 1. Interestingly, the presence of oxygen alters the geometry of the MnO cluster as compared to pure Mn clusters.<sup>17</sup> Moreover, we find that clusters containing up to five MnO units exhibit 2D structures (Fig. 1), and the lowest-lying 3D structures are separated from these by a large energy difference [Fig. 2(a)]. The structural energy difference  $\Delta E_{2\text{D}-3\text{D}}$  for  $(\text{MnO})_4$  and  $(\text{MnO})_5$  clusters are 1.28 and 1.11 eV (equivalent to internal vibrational temperatures of 1650 and 1075 K), respectively. However, the scenario is reversed from the  $(\text{MnO})_6$  cluster (Fig. 1), for which  $\Delta E_{3\text{D}-2\text{D}}$  is 0.61 eV (472 K). The present findings contradict previous theoretical reports, where the PES search was highly biased.<sup>8,9</sup> In contrast, DMC calculations *biased with only FM coupling* predicts a similar geometrical trend for  $x \leq 4$ .<sup>10</sup> The present results are in accordance with the prediction of mass spectra,<sup>18</sup> where Ziemann and Castleman proposed noncubic structural growth, and larger clusters were composed of relatively more stable hexagonal  $(\text{MnO})_3$  and rhombic  $(\text{MnO})_2$  units. Similarly, we also find that the  $(\text{MnO})_3$  cluster is more stable (magic cluster) and serves as the building block for larger clusters. Earlier, it was believed that the small MnO clusters serve as the magnetic core of Mn-based single molecular magnets,<sup>9</sup> this Rapid Communication confirms that there is no such structural resemblance in terms of symmetry. The planar structure of  $(\text{MnO})_4$  (Fig. 1) is substantially different from the magnetic core of  $[\text{Mn}_4\text{O}_3\text{Cl}_4(\text{O}_2\text{CET})_3(\text{py})_3]_2$ ,<sup>1</sup>  $[\text{Mn}_{12}\text{O}_{12}(\text{CH}_3\text{COO})_{16}(\text{H}_2\text{O})_4]$  (Ref. 2) molecular magnets and the oxygen evolving center  $(\text{Mn}_4\text{O}_4\text{Ca})$  in photosystem II.<sup>3</sup> The structural symmetry of  $(\text{MnO})_6$  is very different from that observed in the octahedral  $[\text{Mn}_6(\mu_6\text{-O})(\mu\text{-OR})_{12}]$  molecular complex.<sup>19</sup> However, the structural parameters, such as Mn-O (1.80–2.18 Å), Mn-Mn (2.55–3.10 Å) bond

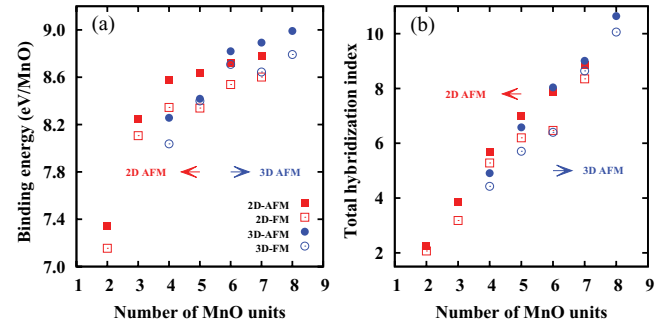


FIG. 2. (Color online) (a) The trend in binding energy shows that the clusters adopt 2D structures until they contain five MnO units, above which they are 3D. The Mn-Mn magnetic coupling is always AFM for the most stable solution. Moreover, the AFM coupling is always favorable over the FM coupling, in both 2D and 3D. (b) Total hybridization index  $\mathcal{H} = \mathcal{H}_{sp} + \mathcal{H}_{pd} + \mathcal{H}_{sd}$  shows a direct correspondence to the energy.

lengths, and Mn-O-Mn angles ( $78^\circ$ – $108^\circ$ ), in these clusters are similar as compared to the molecular magnets (1.85–2.23 Å, 2.77–3.44 Å, and  $94^\circ$ – $137^\circ$ , respectively).<sup>1,2</sup> Also, it should be noted that the Mn-O distance in these clusters already approaches that of the bulk MnO (2.25 Å).

The binding increases substantially due to the presence of oxygen (Fig. 2). This can be explained in terms of electronic configurations. The free Mn atom has  $3d^5 4s^2$  electronic configuration, and, thus, the Mn dimer is weakly bonded.<sup>17</sup> In contrast, our Bader charge analysis<sup>20</sup> shows that Mn atoms lose 1.20e charge to O in  $(\text{MnO})_2$ , which makes binding in these clusters stronger. This amount ( $\sim 1.20e$ ) of charge transfer remains the rule of thumb for all the minimum-energy structures for the stoichiometric MnO clusters. In addition to the covalency, this significant charge transfer suggests an ionic contribution to the Mn-O bonding.

Calculated stability, as measured by  $\Delta E_x = E(\text{MnO})_{x-1} + E(\text{MnO})_{x+1} - 2E(\text{MnO})_x$ , where  $E$  is the total binding energy, shows local peaks for clusters with  $x = 3, 4$ , and 6, in agreement with the experiment.<sup>18</sup> This indicates exceptional stability referring to their magic nature. Clusters with three and four MnO units serve as the building blocks for larger clusters. Two  $(\text{MnO})_3$  cluster units are stacked in 3D for the ground state (Fig. 1), when the similar stacking in 2D (with similar AFM-magnetic ordering) is 0.61 eV higher in energy [Fig. 2(a)]. Similarly, as shown in Fig. 1, an  $(\text{MnO})_3$  unit is stacked in 3D with a distorted  $(\text{MnO})_4$  unit to form the most stable  $(\text{MnO})_7$  cluster. Finally, the  $(\text{MnO})_8$  cluster is formed by staking two  $(\text{MnO})_4$  units.

To understand this morphological transition, we plot the orbital projected density of states for the clusters (Fig. 3). These show a clear trend: The energy spread of the orbitals is higher for the minimum-energy structure and has a larger orbital overlap. For example, an  $(\text{MnO})_4$  cluster has larger orbital spread and has higher  $s$ - $d$  and  $p$ - $d$  hybridizations in 2D compared to the respective optimal 3D structure. In contrast, the situation is reversed for an  $(\text{MnO})_6$  cluster, where the larger spread and higher  $s$ - $d$  and  $p$ - $d$  hybridizations make the 3D structure favorable over the 2D one. The orbital hybridization can be quantified and could explain the cluster morphology.<sup>21</sup>

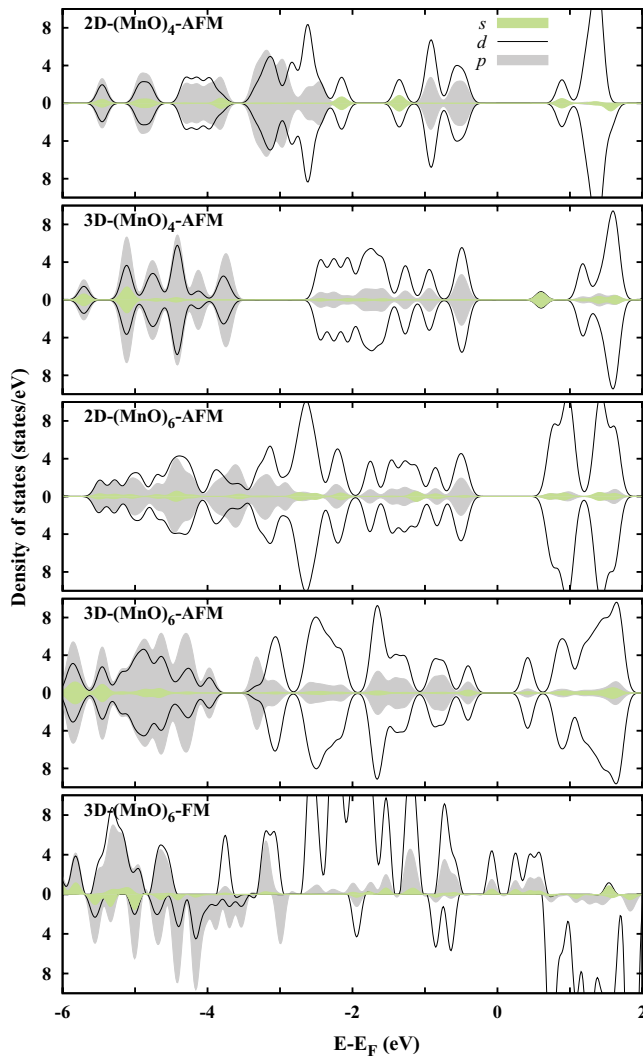


FIG. 3. (Color online) Orbital projected density states summed over all the atoms in the cluster [for 2D and 3D  $(\text{MnO})_4$  and  $(\text{MnO})_6$  clusters in their AFM state; FM state for 3D  $(\text{MnO})_6$  is also shown] show that the minimum-energy structures (both geometric and magnetic) correspond to larger energy spread of the orbitals and higher hybridization. Gaussian smearing (0.1 eV) has been used.

We calculate the  $(k-l)$  hybridization index,

$$\mathcal{H}_{kl} = \sum_I \sum_i w_{ik}^I w_{il}^I, \quad (1)$$

where  $k, l$  are the orbital indices,  $w_{ik}^I (w_{il}^I)$  is the square projection of the  $i$ th Kohn-Sham orbital onto the  $k$  ( $l$ ) spherical harmonics centered at atom  $I$  and integrated over an atomic sphere [radius depends on the atom type, Mn/O (Ref. 22)]. Note that the spin index is inherent. However, unlike gold clusters, in a system with active O- $p$  electrons,<sup>21</sup> in addition to the  $s$ - $d$  hybridization index ( $\mathcal{H}_{sd}$ ), the  $\mathcal{H}_{pd}$  and  $\mathcal{H}_{sp}$  would also play an important role for determining the dimensionality. Indeed, we find [Fig. 2(b)] that the total hybridization index  $\mathcal{H}$  is always higher for the lowest energy structures for the entire size range.

Next, we turn our attention to the magnetic ordering. We find that the Mn atoms in all clusters are AFM coupled. This

gives rise to a net 0 or  $5 \mu_B$  moment for the clusters with even and odd number of MnO units, respectively. It is also interesting to note here that regardless of their dimensional nature, the AFM arrangement is always energetically favorable [Fig. 2(a)]. Experimental evidence of magnetic structure in such clusters is scarce, but the calculated results for the MnO dimer (sextet) is in agreement with the only available experiment.<sup>14</sup> Although the moment is localized on the Mn sites, a small  $p$  polarization (0.02–0.15  $\mu_B$ ) is observed for the oxygen atoms. These results of the magnetic structure are in direct contradiction with the previous results including the DMC calculations.<sup>8–10</sup> As mentioned before, all the previous studies were highly biased and only scanned a small subspace of the PES constrained either by geometrical structure with high symmetry or by FM coupling or constrained by both. We find that the presence of oxygen stabilizes Mn-Mn AFM coupling. For example, the energy difference  $\Delta E(\text{FM-AFM})$  is only  $-0.2$  and  $0.14$  eV for pure  $\text{Mn}_4$  and  $\text{Mn}_6$  clusters, respectively,<sup>17</sup> whereas, this difference substantially increases to  $0.92$  and  $0.67$  eV, respectively, for the  $(\text{MnO})_4$  and  $(\text{MnO})_6$  clusters. It would be interesting to compare the magnetic structure of these clusters with the  $[\text{Mn}_{12}\text{O}_{12}(\text{CH}_3\text{COO})_{16}(\text{H}_2\text{O})_4]$  molecular magnet.<sup>2</sup> The Mn atoms in the inner shell (four  $\text{Mn}^{4+}$ ) and in the outer shell (eight  $\text{Mn}^{3+}$ ) are FM coupled within both of the shells but are AFM coupled between the shells. This is strikingly different from the present  $(\text{MnO})_x$  clusters in the gas phase.

Similar to the morphological stability, the magnetic stability can also be explained in terms of the total hybridization index [Fig. 2(b)] and projected density of states (Fig. 3). Compared to the FM structure, the AFM structure has a larger orbital spread and is accompanied by a higher hybridization index. For example, the 3D-FM structure for  $(\text{MnO})_6$  has sharp  $d$  states (Fig. 3), and in contrast, the  $d$  states for 3D-AFM  $(\text{MnO})_6$  are more widely spread in energy and show larger overlap with O- $p$  states. Calculated total hybridization index  $\mathcal{H}$ , as shown in Fig. 2(b), is much higher in the AFM state (8.04) than in the FM state (6.40) in 3D, confirming the preference of AFM coupling. We restudied the  $(\text{MnO})_4$  and  $(\text{MnO})_6$  clusters using the hybrid PBE0 functional for the exchange correlation, and we should point out that both the structural and the magnetic trends discussed here are found to be unaltered.

Compared to AFM bulk MnO crystal,<sup>7</sup> the overall exchange mechanism is complicated in MnO clusters. The semiempirical Goodenough-Kanamori rules can be employed to understand the Mn-Mn magnetic coupling. In addition to the Mn-O-Mn superexchange mechanism, direct Mn-Mn exchange mechanism is also present in these clusters since the Mn-O-Mn angle is much smaller than  $180^\circ$  (Fig. 1). As we have discussed earlier, pure  $\text{Mn}_4$  is FM with  $\Delta E(\text{FM-AFM}) = -0.2$  eV, i.e., direct exchange prefers FM coupling. When O atoms are introduced, the magnetic structure changes to AFM due to stronger superexchange coupling that prefers AFM Mn-Mn ordering. In contrast, the direct exchange in pure  $\text{Mn}_6$  is already AFM and is further stabilized due to the AFM superexchange when O is introduced. Similar to the ferrimagnetic  $\text{Fe}_4\text{O}_6$  clusters,<sup>23</sup> these stoichiometric MnO clusters also have a very large magnetic exchange (at least 0.11 eV per MnO unit), which is much larger than the Mn-based molecular magnets.<sup>1,2</sup> Therefore, the Curie

temperature of these  $(\text{MnO})_x$  clusters would be much higher than the corresponding AFM bulk MnO ( $\sim 118\text{K}$ ). This can be exploited to tailor new materials.

To summarize, we have demonstrated, through a rigorous and unbiased potential-energy search, that the smaller stoichiometric MnO clusters show unusual 2D structures and that Mn atoms are AFM coupled. Both these features are explained in terms of the inherent electronic structure of these clusters. Present results deviate from the earlier theoretical predictions as those works explored only a small subspace of the potential-energy surface constrained by the high-symmetry structures and ferromagnetic coupling.<sup>8-10</sup> Although the experimental

results on such clusters are scarce, the present results agree well with the limited experimental predictions on the cluster structure and stability.<sup>18</sup> However, there is no experimental evidence on the evolution of magnetic structure; we believe the complementary infrared dissociation spectroscopy<sup>23</sup> will be helpful to confirm both the geometric and magnetic structures of such transition metal-oxide clusters in the gas phase.

M.K. gratefully acknowledges helpful discussions with D. Ceresoli, L.-L. Wang, K. Doll, and D. G. Kanhere. B.S. acknowledges financial support from Swedish Research Links program funded by VR/SIDA.

\*Corresponding author: mukulkab@mit.edu

<sup>1</sup>R. Sessoli, D. Gatteschi, A. Caneschi, and M. A. Novak, *Nature (London)* **365**, 141 (1993).

<sup>2</sup>W. Wernsdorfer, N. Aliaga-Alcalde, D. N. Hendrickson, and G. Christou, *Nature (London)* **416**, 406 (2002).

<sup>3</sup>A. Zouni, H.-T. Witt, J. Kern, P. Fromme, N. Krauss, W. Saenger, and P. Orth, *Nature (London)* **409**, 739 (2001); K. N. Ferreira, T. M. Iverson, K. Maghlaoui, J. Barber, and S. Iwata, *Science* **303**, 1831 (2004); R. Brimblecombe, A. Koo, G. C. Dismukes, G. F. Swiegers, and L. Spiccia, *J. Am. Chem. Soc.* **132**, 2892 (2010).

<sup>4</sup>W. Ruettinger, M. Yagi, K. Wolf, S. Bernasek, and G. C. Dismukes, *J. Am. Chem. Soc.* **122**, 10353 (2000).

<sup>5</sup>F. Jiao and H. Frei, *Chem. Commun.* **46**, 2920 (2010).

<sup>6</sup>J. Li, Y. J. Wang, B. S. Zou, X. C. Wu, J. G. Lin, L. Guo, and Q. S. Li, *Appl. Phys. Lett.* **70**, 3047 (1997); G. H. Lee, S. H. Huh, J. W. Jeong, B. J. Choi, S. H. Kim, and H.-C. Ri, *J. Am. Chem. Soc.* **124**, 12094 (2002).

<sup>7</sup>C. G. Shull and J. S. Smart, *Phys. Rev.* **76**, 1256 (1949); M. D. Towler, N. L. Allen, N. M. Harrison, V. R. Saunders, W. C. Mackrodt, and E. Aprà, *Phys. Rev. B* **50**, 5041 (1994).

<sup>8</sup>S. K. Nayak and P. Jena, *Phys. Rev. Lett.* **81**, 2970 (1998); *J. Am. Chem. Soc.* **121**, 644 (1999).

<sup>9</sup>M. R. Pederson and S. N. Khanna, *Phys. Rev. B* **59**, R693 (1999).

<sup>10</sup>H. Kino, L. K. Wagner, and L. Mitas, *J. Comp. Theo. Nano.* **6**, 2583 (2009).

<sup>11</sup>G. Kresse and J. Hafner, *Phys. Rev. B* **47**, 558 (1993); G. Kresse and J. Furthmüller, *ibid.* **54**, 11169 (1996).

<sup>12</sup>J. P. Perdew, K. Burke, and M. Ernzerhof, *Phys. Rev. Lett.* **77**, 3865 (1996).

<sup>13</sup>P. E. Blöchl, *Phys. Rev. B* **50**, 17953 (1994).

<sup>14</sup>A. J. Merer, *Annu. Rev. Phys. Chem.* **40**, 407 (1989).

<sup>15</sup>L. K. Wagner and L. Mithas, *J. Chem. Phys.* **126**, 034105 (2007).

<sup>16</sup>W. H. Hocking, A. J. Merer, D. J. Milton, W. E. Jones, and G. Krishnamurty, *Can. J. Phys.* **58**, 516 (1980).

<sup>17</sup>M. Kabir, A. Mookerjee, and D. G. Kanhere, *Phys. Rev. B* **73**, 224439 (2006).

<sup>18</sup>P. J. Ziemann and A. W. Castleman, *Phys. Rev. B* **46**, 13480 (1992).

<sup>19</sup>T. C. Stamatatos, K. V. Pringouri, K. A. Abboud, and G. Christou, *Polyhedron* **28**, 1624 (2009).

<sup>20</sup>R. F. W. Bader, *Atoms in Molecules-A Quantum Theory* (Oxford University Press, Oxford, 1990); G. Henkelman, A. Arnaldsson, and H. Jónsson, *Comp. Mater. Sci.* **36**, 354 (2006).

<sup>21</sup>H. Häkkinen, M. Moseler, and U. Landman, *Phys. Rev. Lett.* **89**, 033401 (2002).

<sup>22</sup>For a heterogeneous system, choice of the integrating radius is not unique. However, a choice of  $R_{\text{Mn}} = \langle d_{\text{Mn}-\text{Mn}} \rangle / 2$  and  $R_{\text{O}} = 0.66 \text{ \AA}$  [the covalent radius of oxygen; B. Cordero, V. Gómez, A. E. Platero-Prats, M. Revés, J. Echeverría, E. Cremades, F. Barragán, and S. Alvarez, *Dalton Trans.* 2832 (2008)] captures  $\sim 80\%$  of the electrons.

<sup>23</sup>A. Kirilyuk, A. Fielicke, K. Demyk, G. von Helden, G. Meijer, and T. Rasing, *Phys. Rev. B* **82**, 020405 (2010).